A SPLINE MODEL FOR RV REGISTRATION FROM CARDIAC PET IMAGES

S. Takobana[1,2], A. Adler[2], L. Mielniczuk[1], S. Thorn[1], J. Renaud[1] ,J.N. DaSilva[1], R.S. Beanlands[1], R.A. deKemp[1], R. Klein[1,2]

[1]*University of Ottawa Heart Institute, Ottawa, Ontario, Canada*

[2]*Systems and Computer Engineering, Carleton, Ottawa, Ontario, Canada*

ABSTRACT

Background: The etiology of pulmonary hypertension (PAH) is poorly understood, and is associated with high morbidity and mortality (life expectancy <3 years). PAH leads to progressive enlargement of the right ventricle (RV) with a rapid decline in function. The utility of non-invasive molecular imaging to track PAH progression, evaluate disease etiology and monitor clinical therapy is currently limited by the lack of automated RV image analysis tools.

Objective: To develop a highly automated RV registration, sampling, and analysis tool for human and small animal positron emission tomography (PET) imaging.

Methods: We developed a spline-based model for registering the mid-RV myocardium from a PET uptake image. Model fitting was automated by optimizing a constrained cost function with optional operator intervention.

Inter- and intra-operator variability of FDG PET uptake activity measurements were evaluated using a dataset consisting of 7 PAH and 12 randomly selected non-PAH human subjects. The dataset was processed twice by each of two operators, a novice and an expert. The accuracy of RV cavity volumes and ejection fraction (EF) measurements from cardiac-gated PET images was evaluated by comparing with results from cardiac magnetic resonance imaging (CMR) in 5 PAH patients.

Results: 50% of cases assessed required operator intervention. In intra-operator variability analysis of relative uptake images, the reproducibility coefficient (RPC) for each operator was 5.6% and 6.4% for expert and novice respectively. Inter-operator uptake RPC was 8.2%. RV cavity volumes and EF agreed closely with CMR results (r^2=0.954, n=10 and r^2=0.965, n=5 respectively).

Conclusions: The RV can be automatically registered in uptake PET images and has performance characteristics that are comparable with established left ventricle analysis tools making it suitable for investigating RV molecular and cardiac functions. Additional work is required to improve automation and evaluate molecular function quantification with dynamic imaging.

INTRODUCTION

Pulmonary arterial hypertension (PAH), due to abnormally elevated blood pressure in the pulmonary arteries, can lead to RV (right ventricle) hypertrophy (enlargement) and dysfunction (malfunction) if left untreated [1][2]. PAH is part of a broad category of pulmonary hypertrophy, including left heart diseases, lung diseases or hypoxemia (reduced oxygen in arterial blood) [1][3]. Hypertrophy, occurs when the heart, including the RV, remodels in response to elevated workloads while maintaining stroke volume [4]. Subsequently, hypertrophy and increased pressure leads to dysfunction characterized by decreased cardiac output and poor ventricular contractibility [1][4].

At the molecular level, the etiology and progression of the disease is poorly understood. Furthermore, current anatomical imaging techniques can typically diagnose PAH only at advanced stages, when RV hypertrophy has progressed and cardiac function is reduced. Functional imaging with positron emission tomography (PET) and single photon emission tomography (SPECT) may be able to detect PAH at earlier stages, before mechanical remodeling has occurred. However, due to the thinner RV wall (compared to the left ventricle (LV)), its proximity to the LV, and the limited spatial resolution of these modalities, routine

imaging of non-hypertrophic RVs has been challenging. Due to recent advances in camera and image reconstruction technologies, RV image quality has recently improved to the point where accurate molecular function quantification may be possible. To the best of our knowledge, dedicated software for fast, reproducible, and accurate RV analysis including uptake, cardiac gated and dynamic image analysis does not yet exist.

METHODS

Images acquired from a PET scan were reconstructed in a camera reference frame and roughly traversed the patient transaxially [5]. Images were reoriented to the LV reference frame by iterative fitting of partial ellipses in three orthogonal planes, as previously described [5]. Since the RV is conjoined to the LV it is also reoriented to a standard reference frame as part of the LV reorientation process. The LV was then segmented using a spline model that was automatically fit to the image and could be manipulated by the operator [[4][5][8]. Due to their combined structure, the LV spline was used as a reference to the RV and to estimate the RV shape and size.

The RV region of interest (ROI) was modeled using a spline model [7][8] with a limited number of control points, which roughly define the RV mid-myocardium extending from the septal wall (which was defined in the LV model). Each of these spline points had 1 to 2 degrees of freedom, and could be adjusted automatically or manually to define the general shape of the RV model. ROIs were then determined by interpolating between these points.

Coordinate Systems

In order to describe the spline points' degrees of freedoms, ROI definition, and image sampling, four different coordinate systems must be described:

1) *Cartesian* (x',y',z') – represented the acquired image sampling grid.
2) *Reoriented Cartesian* (x,y,z) – represented the reoriented image sampling grid.
3) *LV spherical-cylindrical (bottlebrush)* – The LV apex region was defined on a spherical (ρ,θ,φ) coordinate system and the LV cavity and base were defined on a cylindrical (ρ,φ,z) coordinate system, relative to the LV long axis (LVLA) [3].
4) *RV pseudo-cylindrical* – RV sampling points were defined using polar coordinate system (φ, r) around the RV long axis (RVLA) in each z plane, where the RVLA curved to remain roughly centered between the septal and RV free wall

Spline control points and interpolated sampling points were located in 3D and their location could be represented in all coordinate systems. In general, RV/LV intersect points were defined on the LV spherical-cylindrical coordinate system so that their movement tracked the LV contours. RV free wall and apical extent were defined in RV pseudo–cylindrical coordinates. After interpolation of the RV sample points in RV pseudo-cylindrical coordinates, they were converted (including image rotation from LV to camera reference frames) into Cartesian coordinates, and tri-linear interpolation was used to sample the image activity in the corresponding RV ROI.

Spline Model

The RV spline model consisted of 12 spline control points with a total of 13 degrees of freedom. Two SA slices defining the mid-cavity (z-slice 8) and the atrium (z-slice 16) were each defined using 5 spline points with a single degree of freedom per spline point as shown in Figure 1A. The notation 1/6 and 2/7 implies that 1 and 2 were points in the cavity slice and 6 and 7 were points in the atrial slice. The direction at which each point was permitted to move is indicated by an arrow beside each control point (Figure 1). The RVLA was interpolated from 3 points: 1 point in each SA plane and from either the RV extent point or RV/LV apex intersect point (points 11 and 12 respectively), which ever had the lowest z coordinate. In the SA planes, RVLA points were defined in the horizontal long axis (HLA) plane (i.e. $\beta = \varphi = 180^{\circ}$, $y=0$) midway between the RV free wall (points 3/8) and the mean of x-components of the anterior and posterior RV/LV intersection points (1/6 and 2/7 respectively),

designated as point *S*. HLA is shown in Figure 1B.

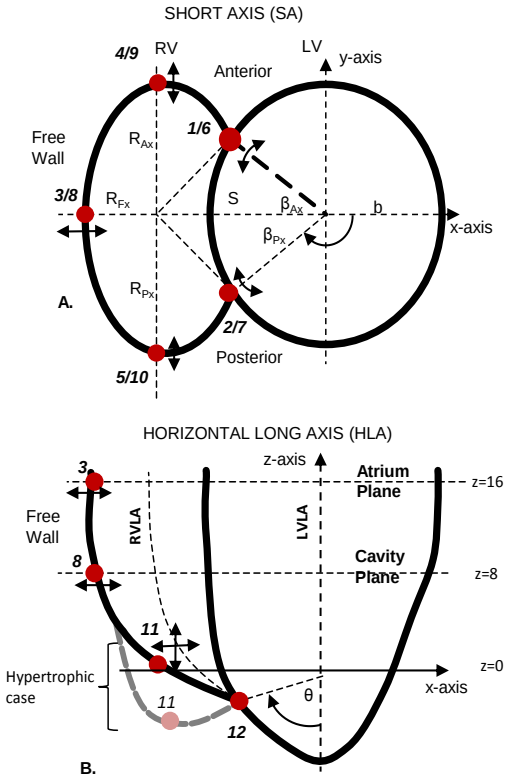

Figure 1: Diagram of the RV spline model relative to the previously described LV spline mode1. Short axis slice (A) and horizontal long axis view of the model in a normal (B) and hypertrophic heart. The control points are shown as red dots and described their degrees of freedom are describes as arrows and in Table 1.

Control points were automatically optimized and were adjustable by an operator using a graphical user interface (GUI). An iterative gradient descent optimization algorithm (fminsearch, Matlab, Natick, MA) was used to adjust a subset of control point parameters (Table 1, Column 3) to automatically register the RV myocardium by minimizing a custom cost function. The RV sample points were interpolated in pseudo-cylindrical coordinates system from the spline points to generate 288 (16 slices by 18 sectors) sample point coordinates.

Table 1: Spline model control points: description, degrees of freedom, and initial location estimate.

Control Point	Degrees of Freedom		Description	Initial Estimate
	Man.	Auto.		
1	1	Ø	Basal Ant. RV/LV intersect	β_{AB} = 120º around LVLA
2	1	Ø	Basal Post. RV/LV intersect	β_{PB}= 240º around LVLA
3	1	1	Basal FW	R_{FB} = 2×*b* from LVLA
4	1	1	Basal Ant.	R_{AB} =*b* from RVLA
5	1	1	Basal Post.	R_{PB} = *b* from RVLA
6	1	Ø	Cavity Ant. RV/LV intersect	β_{AM} = 120º around LVLA
7	1	Ø	Cavity Post. RV/LV intersect	β_{PM}= 240º around LVLA
8	1	1	Cavity FW spline	R_{FM} = 2×*b* from LVLA
9	1	1	Cavity Ant.	R_{AM} = *b* from RVLA
10	1	1	Cavity Post.	R_{PM} = *b* from RVLA
11	2	1 z-only	RV Extent	x = Midway between RV FW and septum z=0
12	1	1	Apex RV/LV intersect	θ=90º

Man. = Manual control by operator, Auto. = Automatic fitting, FW=Free Wall, Ant. = Anterior , Post.=Posterior *b* = LV lateral radius as determined by orientation stage [mm].

Validation and Characterization

The proposed software solution is described in detail, followed by characterization of its appropriateness for human studies with confirmed PAH, human studies without suspicion of PAH, normal rat studies, and studies of a monocrotaline induced PAH rat model.

Inter- and intra-operator variability of FDG PET uptake activity measurements were evaluated using a dataset consisting of 7 PAH and 12 randomly selected non-PAH human subjects. The dataset was processed twice by each of two operators, a novice and an expert.

The accuracy of RV cavity volumes and ejection fraction (EF) measurements from cardiac-gated PET images was evaluated by comparison to results from cardiac magnetic resonance imaging (CMR) in 5 PAH patients

RESULTS

In human studies and hypertrophic rat images the model was able to accurately trace

the RV contours as validated by a human observer, however in normal rat hearts image quality was insufficient to clearly delineate the RV myocardium, and accurate tracking could not be validated. Automatic segmentation was successful in half of the images, with minimal operator intervention required to achieve segmentation in the remainder of images, resulting in a convenient tool that could be used to segment an image in less than 2 minutes per image. In the RV free wall successful automatic segmentation was achieved in nearly all the test images.

Operator dependent variability was evaluated using 19 FDG PET clinical cases consisting of patients with confirmed PAH and patients that were not suspected of having PAH, but were referred due to other cardiac related concerns. Agreement was good with 8.2% relative uptake reproducibility coefficient (95% confidence interval) for inter-operator variability and <6.4% for intra-operator variability.

The accuracy of RV cavity volumes and ejection fractions was excellent as indicated by high correlation (r^2=0.954 and 0.965 for volumes and EF respectively), slopes were not significantly different than unity, low bias, and low RPC (13 mL and 6.3% for volumes and EF respectively) as demonstrated by Blan-Altman analysis[9][10] in Figure 2.

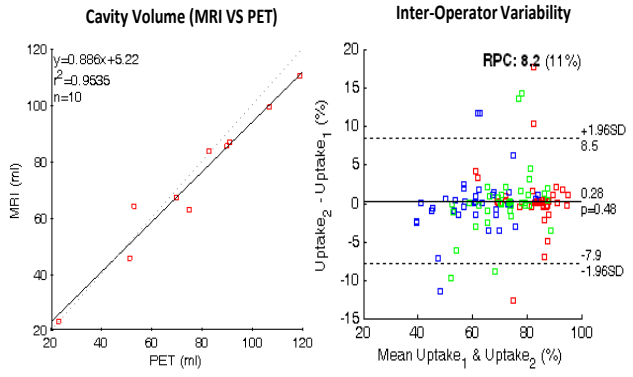

Figure 2:(a) Correlation between cavity volumes from MRI and PET (b) Bland-Altman inter-operator variability analysis for tracer uptake in RV myocardium.

A spline model was developed, validated, and characterized, and was demonstrated to sufficiently registers the RV region of interest semi-automatically. Future validation work with larger data sets is required, as is development of RV specific kinetic analysis tools.

REFERENCES

[1] A. Gomez, D. Bialostozky, A. Zajarias, E. Santos, A. Palomar, M. L. Martinez, and J. Sandoval, “Right ventricular ischemia in patients with primary pulmonary hypertension”, Journal of the American College of Cardiology, vol. 38, no. 4, p. 1137, 2001.

[2] G. Domenighetti, V. Saglini, “Short- and long-term hemodynamic effects of oral nifedipine in patients with pulmonary hypertension secondary to COPD and lung fibrosis, deleterious effects in patients with restrictive disease”, CHEST 1992;102(3):708-714.

[3] J. G. Gomez-Arroyo, L. Farkas, A. A. Alhussaini, D. Farkas, D. Kraskauskas, N. F. Voelkel, and H. J. Bogaard, “The monocrotaline model of pulmonary hypertension in perspective”, American Journal of Physiology - Lung Cellular and Molecular Physiology, vol. 302, no. 4, pp. L363–L369, Feb. 2012.

[4] F. Mannting, Y. V. Zabrodina, and C. Dass, “Significance of Increased Right Ventricular Uptake on 99mTc-Sestamibi SPECT in Patients with Coronary Artery Disease”, Journal of Nuclear Medicine, vol. 40, no. 6, pp. 889–894, Jun. 1999.

[5] R. Klein, J. M. Renaud, M. C. Ziadi, S. L. Thorn, A. Adler, R. S., Beanlands, R. A., deKemp ,“Intra- and inter-operator repeatability of myocardial blood flow and myocardial flow reserve measurements using Rubdium-82 PET and a highly automated analysis program.”, J. Nucl. Cardiol., 2010;17(4):600-616.

[6] J. Chiba, Y. Takeishi, S. Abe, H. Tomoike, “Visualisation of exercise-induced ischaemia of the right ventricle by thallium-201 single photon emission computed tomography”, Heart. 1997 January; 77(1): 40–45.

[7] A.K. Klein, F. Lee, A.A. Amini, "Quantitative coronary angiography with deformable spline models", Medical Imaging, IEEE Transactions, vol.16, no.5, pp.468-482, Oct. 1997.

[8] C. de Boor, *A Practical Guide to Splines*, Springer-Verlag, 1978.

[9] S. Mantha, M. F. Roizen, L. A. Fleisher, R. Thisted, and J. Foss, “Comparing Methods of Clinical Measurement: Reporting Standards for Bland and Altman Analysis”, Anesthesia & Analgesia, vol. 90, no. 3, pp. 593 –602, Mar. 2000.

[10] S. Halligan, “Reproducibility, repeatability, correlation and measurement error”, British Journal of Radiology, vol. 75, no. 890, pp. 193 –194, Feb. 2002.

[11] J. C. Paeng, D. S. Lee, G. J. Cheon, M. M. Lee, J. K. Chung, and M. C. Lee, “Reproducibility of an Automatic Quantitation of Regional Myocardial Wall Motion and Systolic Thickening on Gated 99mTc-Sestamibi Myocardial SPECT”, Journal of Nuclear Medicine, vol. 42, no. 5, pp. 695 –700, May 2001.

[12] S. G. Nekolla, T. Balbach, J. Neverve, F. G. Bengel, M. Schwaiger, "Quantitative cardiac PET imaging: reproducibility in an integrated analysis environment", Nuclear Science Symposium Conference Record, 2000 IEEE , vol.3, no., pp.18/77-18/80 vol.3, 2000.

[13] R. J. Hicks, V. Kalff, V. Savas, M. R. Starling, and M. Schwaiger, “Assessment of right ventricular oxidative metabolism by positron emission tomography with C-11 acetate in aortic valve disease”, The American Journal of Cardiology, vol. 67, no. 8, pp. 753–757, Apr. 1991.